Check for updates

THE AMERICAN SOCIETY OF MECHANICAL ENGINEERS
345 E. 47th St., New York, N.Y. 10017

97-GT-480

The Society shall not be responsible for statements or opinions advanced in papers or discussion at meetings of the Society or of its Divisions or Sections, or printed in its publications. Discussion is printed only if the paper is published in an ASME Journal. Authorization to photocopy material for internal or personal use under circumstance not falling within the fair use provisions of the Copyright Act is granted by ASME to libraries and other users registered with the Copyright Clearance Center (CCC) Transactional Reporting Service provided that the base fee of $0.30 per page is paid directly to the CCC, 27 Congress Street, Salem MA 01970. Requests for special permission or bulk reproduction should be addressed to the ASME Technical Publishing Department.

Copyright © 1997 by ASME All Rights Reserved Printed in U.S.A

Development of a High Pressure Ratio Centrifugal Compressor for 300kW-Class Ceramic Gas Turbine

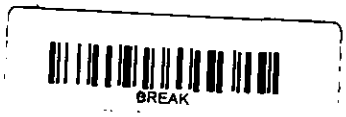

T.Sakai, Y.Tohbe, T.Fujii

Mechanical Engineering Research Department, Akashi Technical Institute

T.Tatsumi

Engineering Department, Industrial Gas Turbine Division

Kawasaki Heavy Industries, Ltd.
Hyogo, Japan

ABSTRACT

Research and development of ceramic gas turbines(CGT), which is promoted by the Japanese Ministry of International Trade and Industry(MITI), was started in 1988. The target of the CGT project is development of a 300kW-class ceramic gas turbine with a 42 % thermal efficiency and a turbine inlet temperature(TIT) of 1350℃. Two types of CGT engines are developed in this project. One of the CGT engines, which is called CGT302, is a recuperated two-shaft gas turbine with a compreseor, a gas-generator turbine, and a power turbine for cogeneration. In this paper, we describe the research and development of a compressor for the CGT302.

Specification of this compressor is 0.89 kg/sec air flow rate and 8:1 pressure ratio. The intermediary target efficiency is 78% and the final target efficiency is 82%, which is the highest level in small centrifugal compressors like this one.

We measured impeller inlet and exit flow distribution using three-hole ysw probes which were traversed from the shroud to the hub. Based on the measurement of the impeller exit flow, diffusers with e leading edge angle distribution adjusted to the inflow angle were designed and manufactured. Using this diffuser, we were able to attain a high efficiency (8:1 pressure ratio and 78% adiabatic efficiency).

NOMENCLATURE

π_t	Total pressure ratio (total-to-total)
π_s	Static pressure ratio (total-to-static)
η_t	Adiabatic efficiency (total-to-total) [%]

Subscripts

a	Compressor inlet
1	Impeller inlet
2	Impeller exit
4	Diffuser exit
shr	shroud wall
hub	hub wall

The pressure ratio is defined as follows.

$\pi_t = P_t / P_{ta}$

$\pi_s = P_s / P_{ta}$

P_t	Total Pressure at a measuring station
P_s	Static Pressure at a measuring etation
P_{ta}	Total pressure at compressor inlet

INTRODUCTION

The Japanese CGT development program, which was started in 1988 as a part of its "New Sunshine Project" with the aim of aaving energy and protecting the environment, came to an intermediate appraisal in 1994.

Kawasaki Heavy Industries (KHI) is taking part in this program and has been developing CGT, which is named the CGT302 (300kW regenerative two-shaft ceramic research gas turbine engine) jointly with Kyocera Corporation (KC) for the ceramic components and Sumitomo Precision Products (SPP) for recuperator. Table.1 shows the target performance of the CGT302. We have been steadily striving to realize the target performance and will continue to do so.

Compressors for the CGT302 engine are single-stage centrifugal compressors. Fig.1 shows the current status of centrifugal compressor efficiency. Our target, which is 82% adiabatic efficiency and 8:1 pressure ratio, represents the highest performance in small compressors of this type. In

Presented at the International Gas Turbine & Aeroengine Congress & Exhibition
Orlando, Florida — June 2–June 5, 1997

Downloaded from http://asmedigitalcollection.asme.org/GT/proceedings-pdf/GT1997/78682/V001T03A093/2408780/v001t03a093-97-gt-480.pdf by guest on 28 May 2022

order to achieve high efficiency at high pressure ratio, we carried out compressor performance tests combining various impellers and diffusers, then took detailed measurements of the internal air flow at the impeller inlet and exit. After the results of these measurements were studied, new diffusers were designed and manufactured. This paper describes the development of the compressor, the procedure for taking detailed measurements, and the test results obtained.

Table 1 Target performance of the CGT302

Item	Unit	Target
Output Power	kW	300
Thermal Efficiency	%	42
Turbine Inlet Temperature	℃	1,350
Pressure Ratio		8
Air Flow Rate	kg/s	0.89
Compressor Efficiency	%	82
Turbine Efficiency	%	85.5
Heat Exchanger Efficiency	%	80
GGT Rotor Speed	rpm	76,000
PT Rotor Speed	rpm	57,000

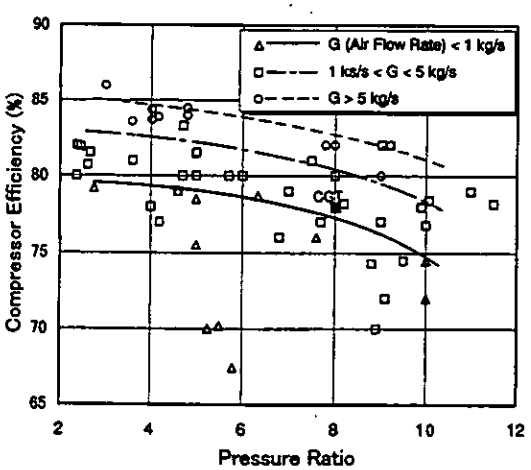

Fig.1 Current Status of Centrifugal Compressor Efficiency

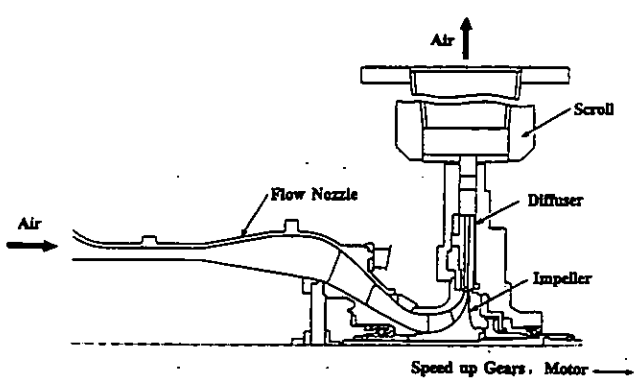

Fig.2 Cross Section of the Compressor Test Rig

COMPRESSOR TEST RIG

A cross-sectional view of the compressor test rig in which impellers and diffusers were set up is shown in Fig.2. This test equipment is driven by an electric motor (maximum rotational speed of 3,600rpm), and the rotational speed can be increased by two speed up gears (gear ratio of 2.5:1 and 10:1). Air flow rate and compressor exit pressure are adjusted by valves in the compressor exit manifold. Air flows from the intake nozzle in the axial direction, then through the impeller, diffuser, and scroll, finally flowing out in the radial direction.

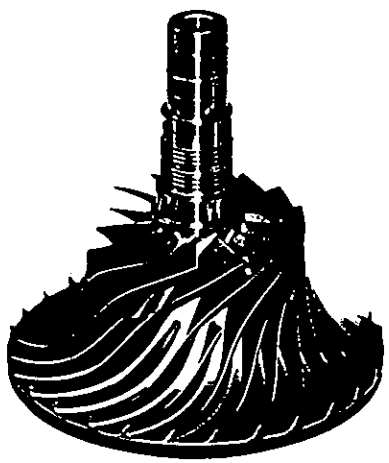

Fig.3 View of E impeller

Table 2 Specification of E Impeller

Rotational Speed (rpm)	76,000
Number of Blade	14+14(Splitter)
Inducer Hub Diameter (mm)	38
Inducer Shroud Diameter (mm)	92
Tip Diameter (mm)	160
Inducer Hub Angle (deg)	43.6
Inducer Shroud Angle (deg)	64.3
Backward Angle (deg)	44

IMPELLER DESIGN

The impeller was milled out of a titanium alloy (Ti-6246) block. Fig.3 shows a test impeller (E impeller), while Table 2 shows the main specifications of the E impeller. Prior to designing the impeller, performance was predicted, and the approximate dimensions of the impeller inlet, exit, and diffuser exit were determined. Then computational flow analysis was carried out to improve aerodynamic performance and while analyzing the stress of the impeller blades and disk was executed to reduce the stress.

The aerodynamic analysis of the impeller was carried out with a code that solves three-dimensional, compressible

Downloaded from http://asmedigitalcollection.asme.org/GT/proceedings-pdf/GT1997/78682/V001T03A093/2408780/v001t03a093-97-gt-480.pdf by guest on 28 May 2022

Eular equations. The grid used for the calculation has 10×75×10 points in the blade-to-blade, throughflow, and hub-to-shroud directions. Since geometric parameters such as meridional shape, blade angle, blade thickness, splitter blade leading edge position, and splitter blade shape affected each other, the impeller shape was repeatedly corrected to improve the air flow pattern. The following was especially noticed with this impeller design.

- Decreasing the maximum Mach number on the inducer shroud side by varying the blade angle distribution.
- Uniforming deceleration on the inducer hub side by correcting the hub meridional shape

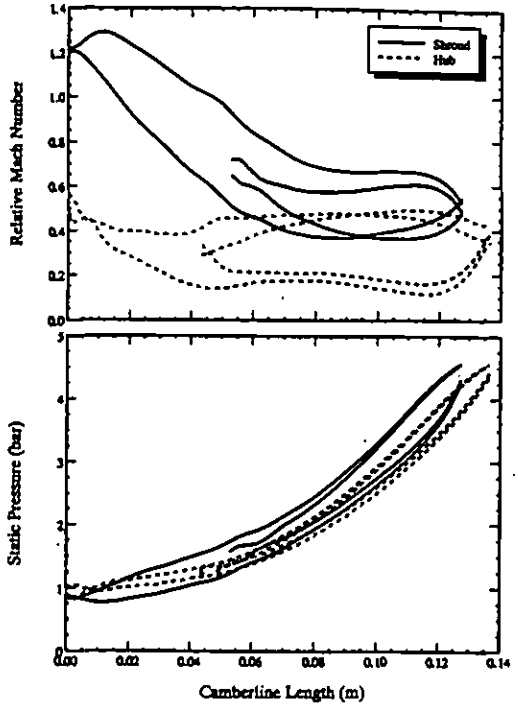

Fig.4 Aerodynamics Analysis Results

Fig.4 shows the E impeller aerodynamic analysis result.

Stress of impeller blades and disk was analyzed using the boundary element method, the model of which is symmetrical around impeller rotating axis. The E impeller stress analysis result is shown in Fig.5, where the value is normalized by the maximum. The maximum stress was acceptable.

EXPERIMENTAL EQUIPMENT AND PROCEDURES

In order to achieve a high efficiency at high pressure ratio, we took detailed measurements of the internal air flow (total pressure and flow angle) at the impeller inlet and exit using miniature three-hole yaw probes. These probes were traversed in the radial direction at impeller inlet and in the

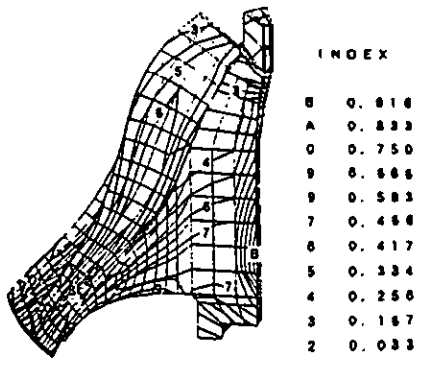

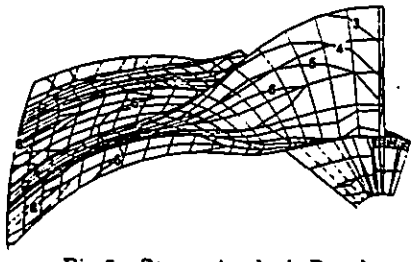

Fig.5 Stress Analysis Results

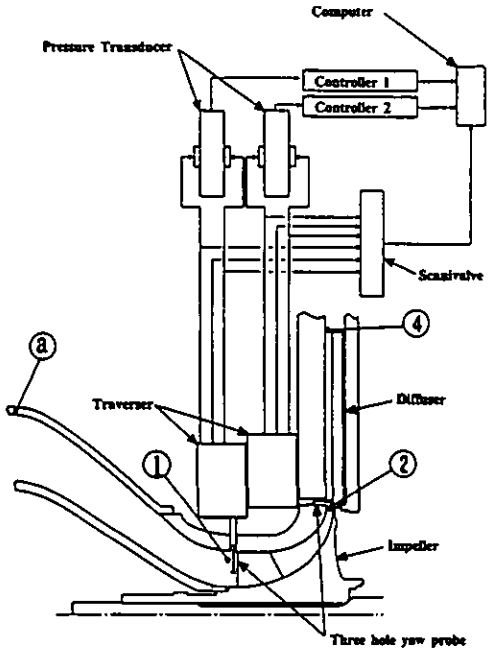

Fig.6 Measurement Locations and Measurement System

axial direction at impeller exit and could be rotated around the stem. Pressure data were acquired after the yaw probes had been rotated to the direction in which the difference among pressures of side holes was zero. The purpose of these probes was to measure the time-averaged flow angle and total pressure. A vaneless diffuser was used in this measurement to assess the impeller's performance because diffuser vanes are known to affect the air flow

Downloaded from http://asmedigitalcollection.asme.org/GT/proceedings-pdf/GT1997/78682/V001T03A093/2408780/v001t03a093-97-gt-480.pdf by guest on 28 May 2022

characteristics at impeller exit. This measurement location (station a-4) and the measurement system is shown in Fig.6, and the instrumentation is summarized in Table 3. The measurement location was 4mm upstream of the impeller leading edge in the axial direction (impeller inlet) and where radius ratio R/R2 was 1.04 (impeller exit). The height of flow path was 27mm at the impeller inlet and 6mm at the impeller exit.

Table 3 Location of Measurement

Location	Flow Variable	Instrument Type	Quantity
Compressor	Total Pressure	Cobra Probe	3
Inlet	Total Temperature	Resistance Temp. sensor	3
(Station a)	Air Flow Rate	Flow Nozzle	
Impeller	Air Flow Angle	Traversing Yaw Probe	1
Inlet	Total Pressure	Traversing Yaw Probe	1
(Station 1)	Static Pressure	Shroud Wall Tap	3
Impeller	Air Flow Angle	Traversing Yaw Probe	1
Exit	Total Pressure	Traversing Yaw Probe	1
(Statioa 2)	Static Pressure	Shroud Wall Tap aod	3
		Hub Wall Tnp	3
Diffuser	Total Pressure	Cobra Probe	3
Exit	Static Pressure	Shroud Wall Tap	3
(Station 4)	Total Temperature	Probe with Thermocouple	3

The yaw probes were calibrated in a wind tunnel in advance to clarify the relation between the characteristics of yaw probe and total pressure, static pressure and air flow angle. As a result of this calibration, total pressure and air flow angle was corrected. To determine static pressure, we use the values calculated from yaw probe coefficient at impeller inlet and the shroud wall pressure at impeller exit because the air flow path bends on the meridional plane at impeller inlet and remains straight at impeller exit.

MEASUREMENT RESULTS

We acquired traverse data up to 90% of the design speed. The pressure ratio at impeller exit with the combination of E impeller and vaneless diffuser is shown in Fig.7. The measurement results under 4 operating conditions at 70% and 90% speed are described in this paper.

Fig.8 shows relative air flow angle and absolute meridional velocity distribution between hub-to-shroud at impeller inlet. The meridional velocity on the shroud side tends to be higher than on the hub side. The slope of the blade leading edge angle curve is nearly equal to the slope of the relative flow angle curve at 90% speed near surge. This indicates that design of impeller incidence is suitable.

Fig.9 shows absolute air flow angle and Mach number distribution between hub-to-shroud at impeller exit. The air flow angle is lower near both walls, and the differences are

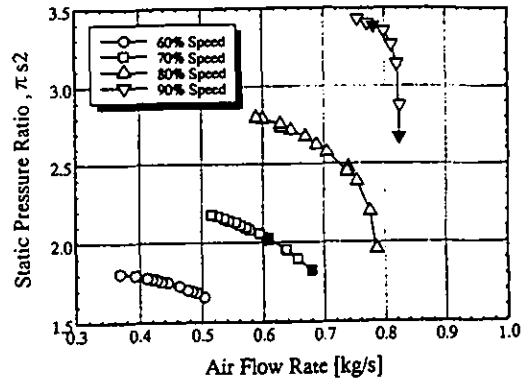

Fig.7 Compressor Characteristics with E impeller and Vaneless Diffuser

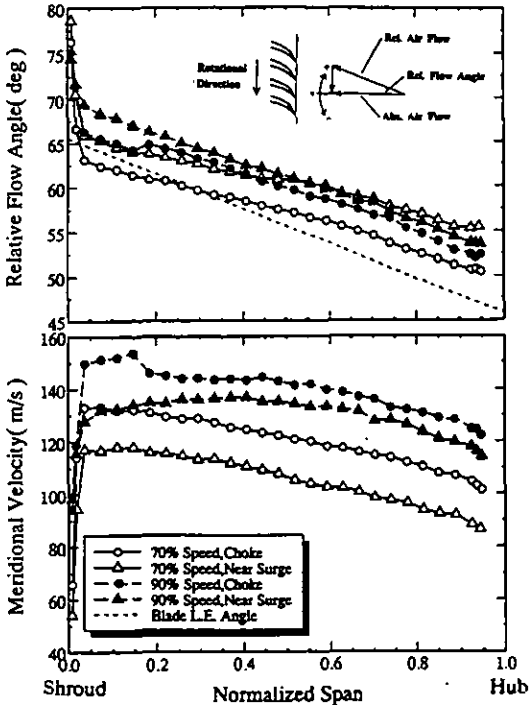

Fig.8 Impeller Inlet Traverse Results

greater than 30 degrees at choke. Peak of the air flow angle leans to the hub side of the flow path and the location of the peak remains relatively unchanged at 70% speed, while it moves to the shroud side at 90% speed as the air flow rate decreases. Near surge, counter-flow region appears near the shroud wall. The absolute flow angle and Mach number distribution indicate that the larger boundary layer development on the shroud wall than on the hub wall and the main flow leans to the hub side. These results suggest that it is necessary to design impellers without generating a counter-flow near the shroud wall and by pushing the main flow to the shroud side.

Downloaded from http://asmedigitalcollection.asme.org/GT/proceedings-pdf/GT1997/78682/V001T03A093/2408780/v001t03a093-97-gt-480.pdf by guest on 28 May 2022

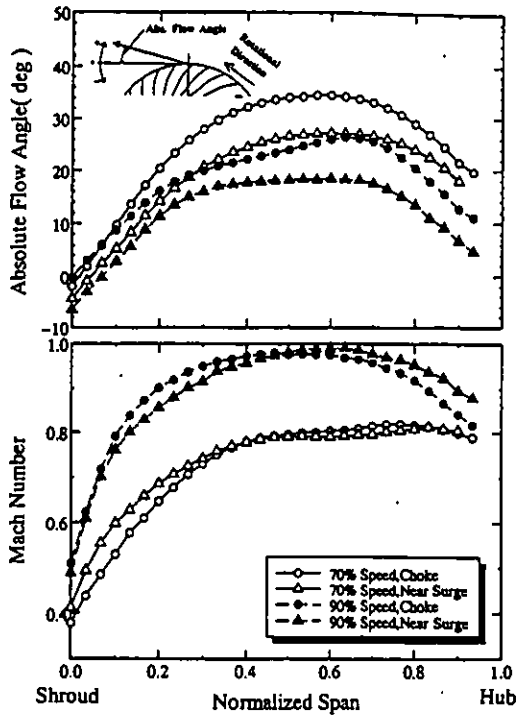

Fig.9 Impeller Exit Traverse Results

DIFFUSER DESIGN

Utilizing the detailed flow measurement results to assess the flow distribution in the hub-to-shroud direction at impeller exit, we designed and manufactured CB-9 channel diffuser whose leading edge angle distribution is nearly equal to the inflow angle. CB-9 diffuser is based on CB-6 channel diffuser with which the test result was not so bad. The number of vanes, the maximum leading edge angle and the divergence angle in the direction of the width of CB-9 diffuser are the same as in CB-6, and the flow path height is 6 mm. The vane side wall was milled out by a cutter with a spherical point. We selected a track of the vane side wall having the leading edge angle that most closely matched the inflow angle of the diffusers whose throat area was equal to that of CB-6.

Tips of the vane island close to both walls were cut off because they had negative vane angles. Table 4 shows the specifications of CB-9 channel diffuser, CB-6 channel diffuser and PB-1 pipe diffuser. Fig.10 shows a comparison of the vane leading edge angle of CB-9 and PB-1 diffuser, and the air inflow angle. Fig.11 provides the illustrations of these diffusers. The shape of CB-9 diffuser leading edge is similar to that of PB-1 pipe diffuser and the leading edge angle of CB-9 matches the air flow angle better than that of PB-1.

Table 4 Specification of Diffusers

	CB-6, CB-9	PB-1
Type	Channel	Pipe
Inlet Vane Angle (deg)	15	14.1
Number of Vane or Pipe	19	17
Divergence Angle (deg)	8	6
Vaneless Ratio	1.05	1.05

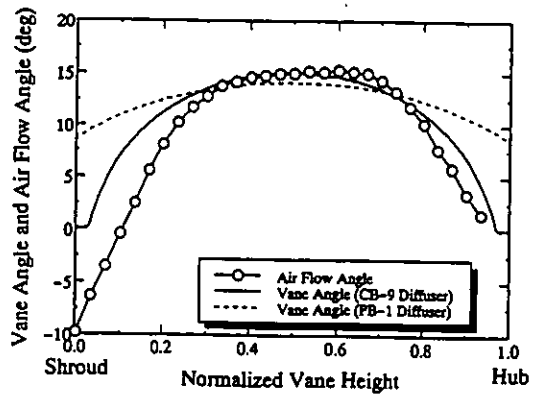

Fig.10 Vane Leading Edge Angle Distribution of Diffusers

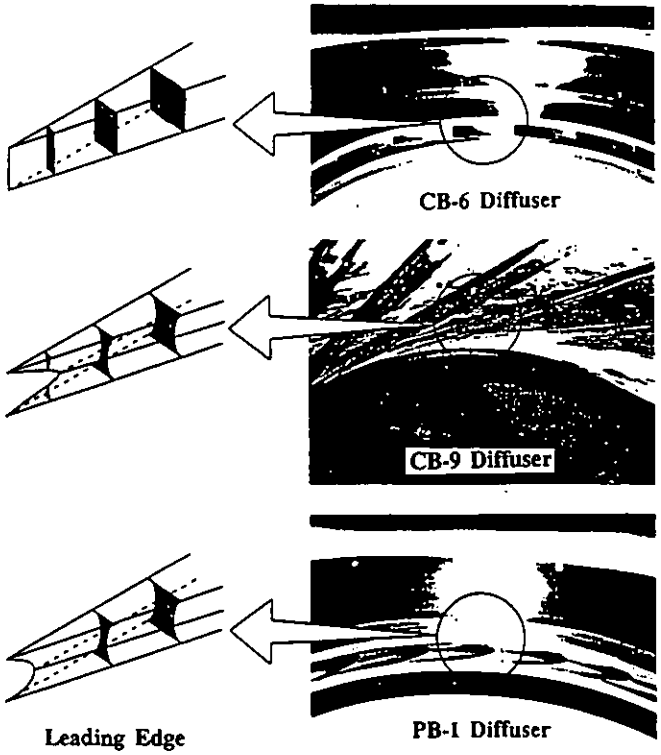

Fig.11 View of Diffusers

COMPRESSOR PERFORMANCE TEST RESULTS

Fig.12 shows the test results obtained with the combination of E impeller and CB-9 diffuser and the one of E

Downloaded from http://asmedigitalcollection.asme.org/GT/proceedings-pdf/GT1997/78682/V001T03A093/2408780/v001t03a093-97-gt-480.pdf by guest on 28 May 2022

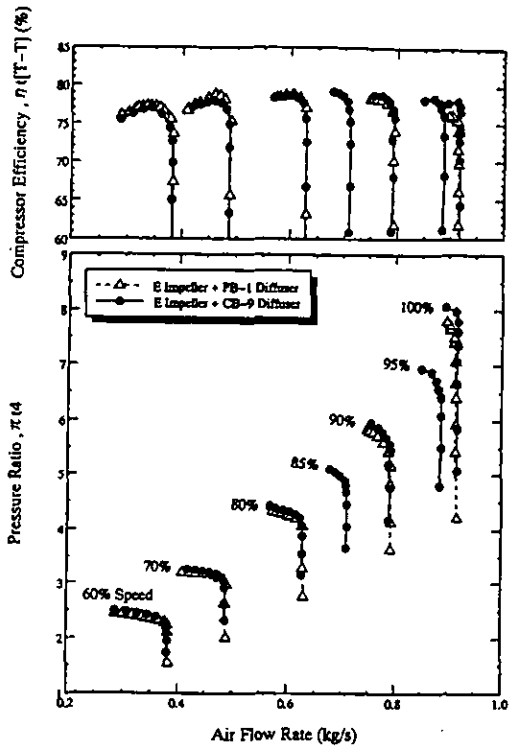

Fig.12 Compressor Performance Test Results

impeller and PB-1 diffuser. At 100% speed, we attained 8:1 total-to-total(t-t) pressure ratio and 78% t-t adiabatic efficiency with CB-9 diffuser. The efficiency of CB-9 diffuser was about 2% higher than that of PB-1 diffuser. The efficiency of CB-9 diffuser is lower than that of PB-1 at less than 70% speed, although the opposite is true at more than 70% speed. These results show that adjusting the distribution of the diffuser leading edge angle in the hub-to-shroud direction to the air inflow angle will lead to good efficiency at the design rotational speed. However, because the diffuser characteristics at 100% speed moved too much to the high flow rate side, choke at the inducer arose, and the compressor operating range was very limited. If the throat area is somewhat narrowed, it is expected that the operating range will be wider.

CONCLUSIONS

Detailed measurements were taken of the internal air flow (air flow angle and pressure) at impeller inlet and exit by traversing miniature three-hole yaw probes in the hub-to-shroud direction. Although such measurements are very difficult because of the low height of the air flow path(6 mm) and the high pressure ratio (8:1) and high temperature(300℃) at impeller exit, good results were obtained.

As a result of the detailed measurements taken at impeller inlet, it was found that there is little difference between the blade angle of the impeller leading edge and the air inflow angle.

At impeller exit, the main flow leans to the hub wall and is inclined to move to the shroud side as the air flow rate decreases. Moreover, it was clarified that back flow existed near the shroud wall at near surge, which means that we must design impellers which push the main flow to the shroud side.

On the basis of the detailed measurements taken at impeller exit, new diffusers whose leading edge angle distribution are nearly equal to the inflow angle distribution were designed and manufactured, and we were able to attain a high compressor adiabatic efficiency.

ACKNOWLEDGMENTS

The present study was carried out under the Japanese CGT R&D program conducted by New Energy and Industrial Technology Development Organization(NEDO). The authors would like to express their deep appreciation to the Agency of Industrial Science and Technology of the Ministry of International Trade and Industry(MITI) and NEDO for making this study possible and for permitting this paper to be published.

REFERENCES

1. Y. Ichikawa et al., 1997, "Current Status of CGT302 (Progressing to final phase)", ASME 97-GT
2. D. Eckardt, "Instantaneous Measurements in the Jet-Wake Discharge Flow of a Centrifugal Compressor Impeller", Journal of Engineering for Power, Trans.ASME, Series A, Vol.97, No.3, July 1975, pp.337-346
3. J. D. Denton and U. K. Singh, "Time Marching Methods for Turbomachinery Flow Calculation", VKI Lecture Series on Transonic Flows for Turbomachinery, 1979

Downloaded from http://asmedigitalcollection.asme.org/GT/proceedings-pdf/GT1997/78682/V001T03A093/2408780/v001t03a093-97-gt-480.pdf by guest on 28 May 2022